ELSEVIER

European Journal of Pharmaceutics and Biopharmaceutics 50 (2000) 307–318

European Journal of Pharmaceutics and Biopharmaceutics

www.elsevier.com/locate/ejphabio

Research paper

Interactions between hydroxypropylcelluloses and vapour/liquid water

Carmen Alvarez-Lorenzo, Jose Luis Gómez-Amoza, Ramón Martínez-Pacheco, Consuelo Souto, Angel Concheiro*

Departamento de Farmacia y Tecnología Farmacéutica, Facultad de Farmacia, Universidad de Santiago de Compostela, Santiago de Compostela, Spain

Received 3 January 2000; accepted 7 May 2000

Abstract

Understanding of the uptake of water vapour or liquid water by cellulose-based polymers is important because of the influence of these processes on many of the biologically or technologically relevant properties of these polymers. In this work we studied these processes in the cases of twelve hydroxypropylcelluloses with low or medium-high degrees of substitution (L-HPCs and HPCs, respectively), characterization of which showed significant differences in structural and physical parameters (substitution pattern, crystallinity, particle size, specific surface area, and intraparticular porosity). Water vapour sorption–desorption isotherms determined to characterize the uptake of water vapour were fitted well by the Young–Nelson model, the optimized parameters of which indicated that at all relative humidities the capacity to bind water vapour as a surface monolayer is greater for HPCs than L-HPCs, but the capacity to absorb water vapour internally is greater for L-HPCs than HPCs. Guggenheim–Anderson–deBoer (GAB) models fitted the sorption–desorption isotherms less well. Differential scanning calorimetry (DSC) experiments showed all sorbed water vapour to be held as non-freezing water. Isoperibol microcalorimetry experiments carried out to investigate interactions with liquid water showed enthalpies of hydration/dissolution of between -62.86 and -71.35 J g^{-1} for L-HPCs and between -82.95 and -99.80 J g^{-1} for HPCs, and DSC showed average numbers of non-freezing water molecules per polymer repeat unit of 2.65–4.19 for L-HPCs and 18.10–22.42 for HPCs. DSC characterization of the kinetics of the water uptake by 10 mg compacts obtained by direct compression of hydroxypropylcelluloses showed faster uptake by L-HPC compacts than by HPC compacts, among which there were significant differences in capacity for diffusive uptake. The explanations of the above differences in terms of the different substituent contents, particle sizes and porosities of the HPCs is supported by multiple linear regression analyses.

Keywords: Hydroxypropylcellulose; Moisture sorption analysis; Substitution; Microcalorimetry; Differential scanning calorimetry; Water behaviour

1. Introduction

Polysaccharides are generally hydrophilic and interact strongly with polar liquids and vapours through hydrogen bonds. Crystalline polysaccharides typically exist in anhydrous and hydrated forms, both of which interact with water vapour primarily by adsorption and deliquescence mechanisms [1,2]. The Langmuir, Brunauer–Emmet–Teller (BET) and Guggenheim–Anderson–deBoer (GAB) equations are usually applied to describe isothermal water vapour adsorption data [2]. Amorphous saccharides usually absorb water into their bulk structure, which may cause crystallization or, in the case of large polysaccharides, the cleavage of polymer–polymer bonds, the creation of water–polymer bonds, the separation of polymer chains, swelling, and finally the dispersion of polymer chains in the medium [3]. Transitions between anhydrous and hydrated polysaccharides are usually studied by water-vapour sorption techniques [1,4] and by thermal analytical techniques such as differential scanning calorimetry (DSC) [3,5,6]. The uptake of water vapour by a solid material depends on its chemical structure and physical properties, and on the ambient relative humidity, which determines the equilibrium moisture content of any given solid [1,7].

The Young–Nelson [4] model, originally developed to account for water uptake by wheat, assumes that when a dry material is exposed to moisture, water molecules first adsorb onto its surfaces to form a monomolecular layer which is subjected to both surface binding and diffusional forces, the latter tending to cause the transfer of moisture into the material. If the water vapour pressure is reduced, water molecules at the surface must be removed before

* Corresponding author. Departamento de Farmacia y Tecnología Farmacéutica, Facultad de Farmacia, Universidad de Santiago de Compostela. 15706 Santiago de Compostela, Spain. Tel.: +34-981-594627; fax: +34-981-547148.

E-mail address: ffancon@usc.es (A. Concheiro).

0939-6411/00/$ - see front matter
PII: S0939-6411(00)00104-1

diffusional forces pull moisture out of the interior of the material. Beyond a certain level of uptake, water in amorphous solids may form condensed phases with solvent-like properties because of the saturation of binding sites. It has also been proposed that water sorption by amorphous polysaccharides may be described using conventional solution theories such as Raoult's law and Henry's law, but observed positive deviations from the ideal behaviour at low-to-moderate humidities [2] indicate that strong attraction between the polysaccharide and water molecules outweighs the homointeractions [8].

In polymer research, it is frequently assumed that water of hydration in macromolecules can be classified in three types: free water, which undergoes thermal phase transitions similar to those of bulk water; freezing bound water, which exhibits a melting/crystallization temperature different from that of bulk water; and non-freezing water, which does not exhibit a detectable phase transition in the neighbourhood of the melting temperatures of bulk water. Non-freezing water is regarded as being held more tightly by the hydrophilic groups of the polymer backbone than freezing bound water, which is considered to be in equilibrium with both free and non-freezing water [3,6,9,10]. DSC has proved invaluable for quantification of the amounts of water bound by microcrystalline celluloses (MCCs) [8], hydroxyethylcelluloses (HECs) [6] and hydroxypropylmethylcelluloses (HPMCs) [3,11,12], and flow calorimetry [7] and conventional microcalorimetry [3] allow these quantities to be related to the thermodynamics of dissolution.

Sorbed water can markedly change the physical and chemical properties of polysaccharides, and can thus have a significant impact upon their uses [5,13]. For example, sorbed water can accelerate hydrolytic degradation, isomerization and/or crystallization processes, all of which are usually undesirable for food processing and for the preservation of biological activity in freeze-dried pharmaceutical preparations [1,5]. Water sorption by polysaccharides also plays a dominant role in the seasonal acclimatization of living organisms to environmental stresses such as drought, sub-zero temperatures or high salinity [14]. In the case of cellulose ethers, interactions with water vapour affect the flow [15,16] and compaction [12,17] properties of the polymer, as well as its physical and chemical stability [18] and the rate at which drugs are released from conventional solid drug dosage forms with cellulose ether excipients [8,17]. They also affect the transmission of light through optical fibres made of cellulose ether films [19].

Interactions with liquid water contribute to control the conformation of the polymer in solution and hence the viscosity of polymer solutions, the adsorption of the polymer at solid–liquid and liquid–liquid interfaces, and its efficacy as a stabilizer in liquid drug dosage forms [20,21] or in suspensions of semiconductor particles [22,23]. In addition, the nature and extent of water–polymer interactions govern the formation, upon contact with water, of the cellulose ether gel layer that determines the rate at which the drug is released from many controlled release oral drug dosage forms [24,25].

In this article we report the results of a study of water uptake by hydroxypropylcellulose, a cellulose ether for which there is little available information on its interactions with water in spite of its widespread use in controlled drug delivery [8,26] and its applications in electrophoresis [27], optochemical sensors [19] and semiconductor systems [22,23]. In order to investigate both the effects of characteristics that have been considered in studies of other cellulose ethers, such as particle size or degree of substitution (DS) [15,17], and those of potentially relevant characteristics such as microstructure, crystallinity and substitution pattern [1,7,28–30], twelve different varieties of hydroxypropylcellulose produced by three different manufacturers were studied: five insoluble varieties with low DS (L-HPCs) and seven soluble varieties with medium-high DS (HPCs). These products were characterized as to their molecular, granulometric and microstructural properties, and experiments were performed to identify the mechanisms by which they take up water vapour or interact, in powder and compacted form, with bulk water, and the variables determining the extent and rate of these processes.

2. Materials and methods

2.1. Materials

Low-DS hydroxypropylcelluloses (L-HPCs): varieties LH-11 (batch 503078), LH-20 (405117), LH-21 (506157), LH-22 (301018) and LH-31 (502032) from Shin-Etsu Chemical Co. Ltd. (Tokyo, Japan). Medium/high-DS hydroxypropylcelluloses (HPCs) of nominal viscosity 100–400 mPa s: varieties Klucel®GF (batch FP10-10293) from Aqualon (Hercules Inc., Wilmington, DE), and Nisso® M (batches BJ-031, DC-631 and JD-471) from Nippon Soda Co. (Tokyo, Japan). HPCs of nominal viscosity 1000–4000 mPa s: varieties Klucel® MF (batch 7857) from Aqualon, and Nisso® H (batches BJ-141 and JE-161) from Nippon Soda Co.

2.2. Characterization of the polymers

2.2.1. Degree of substitution and molar substitution

The substitution patterns of the various hydroxypropylcelluloses were evaluated by ^{13}C NMR spectroscopy of their hydrolysates, as follows. First, 1.0 g of polymer was added to 30 ml of 6 M sulphuric acid and stirred for 1.5 h at 20°C. The mixture was then made up to 90 ml with deionized water, autoclaved at 2 atm for 1 h, cooled, neutralized with barium carbonate, filtered, and concentrated to 2 ml in a rotary evaporator at 40°C. A 1 ml sample was then made up to 2 ml with D_2O and centrifuged at $3575 \times g$ for 5 min, and 1 ml of the resulting supernatant was analyzed by NMR spectrometry in a Bruker AMX-300 apparatus at 75 MHz. All shifts were referred to chromium(III) acetylacetonate (3

mg ml^{-1} in dimethylsulphoxide) at 40 ppm. Spectra were interpreted and degree of substitution (DS) and molar substitution (MS) were estimated as per Lee and Perlin [31] and Alvarez-Lorenzo et al. [32].

2.2.2. Crystallinity

Crystallinity was evaluated by infrared spectrophotometry using a Bruker IFS 66V FTIR apparatus with an Nd:YAG laser and a germanium detector cooled with liquid nitrogen. Crystallinity was quantified as the ratio between the absorbance values recorded at 1370 and 2900 cm^{-1} in 32-scan spectra of samples incorporated in KBr discs [33].

2.2.3. Particle size analysis

Martin diameters were determined on the basis of measurement of 625 particles of each hydroxypropylcellulose under an Olympus BH-2 light microscope. The geometric mean and geometric standard deviation (SD) were determined after logarithmic transformation of the data.

2.2.4. Specific surface area and microporosity

Nitrogen adsorption experiments were carried out in a Micromeritics ASAP 2000 apparatus using samples that had been degasified by being kept for 8 h at 70°C and 10^{-3} mmHg. Nitrogen adsorption at 77 K was measured over the relative pressure range 0.06–0.99. Each polymer variety was run in duplicate.

Specific surface area (S_{BET}) was estimated from the volume of a nitrogen monolayer (V_m, calculated from the BET equation) using the expression

$$S_{BET}(m^2g^{-1}) = 4.37(m^2cm^{-3}) \times V_m(cm^3g^{-1}) \quad (1)$$

Following Barret et al. [34], mean pore size and micropore volume were estimated from the nitrogen desorption isotherms on the assumption that equilibrium between the gas phase and the adsorbed phase during desorption is determined by (1) physical adsorption on the pore walls and (2) capillary condensation in the inner capillary volume; a numerical method was used to solve the Barret et al. [34] equation

$$\Delta V_p = R_n \times (\Delta V_c - C \times \Delta t \times \Sigma S_p) \quad (2)$$

where ΔV_p is the actual pore volume emptied in the desorption step, C is a correction factor to allow for the change in curvature of the pore wall as pore size changes, ΣS_p is the sum of the surface areas over all the desorption steps, and R_n is calculated using the expression

$$R_n = r_p^2/(r_k + t)^2 \quad (3)$$

where r_p is the actual pore radius, r_k is the mean capillary condensate radius, and t is the decrease in multilayer thickness during the desorption step.

2.2.5. Sorption–desorption of water vapour

Plots of equilibrium moisture content against relative humidity at 20°C were constructed using 1.5 g samples stored for 3 weeks at constant relative humidities of 0, 18.8, 47.2, 70.4, and 93.9, controlled with mixtures of water and sulphuric acid [35]. Here after the values of the relative humidity will be used as per unit, i.e. 0.00, 0.188, 0.472, 0.704, and 0.939. Samples used for sorption isotherms were previously desiccated and weighed, and samples used for desorption isotherms were previously desiccated, weighed and hydrated by storage at a relative humidity of 0.939. Moisture contents were calculated by weight difference with respect to the pre-treatment desiccated sample.

For Young–Nelson [4] analysis, non-linear and stepwise multiple regression analyses (Statgraphics® v. 7.0) were used as proposed by Nokhodchi et al. [12] to fit the sorption and desorption data with equations of the form

$$M_s = A(\theta + \beta) + B\theta H \quad (4)$$

$$M_d = A(\theta + \beta) + B\theta H_{max} \quad (5)$$

respectively, where M is moisture content, the subscripts 's' and 'd' indicate sorption and desorption respectively, H is relative humidity

$$\theta = H/[H + E(1 - H)] \quad (6)$$

and

$$\beta = -\frac{EH}{E - (E-1)H} + \frac{E^2}{E-1}\ln\left(\frac{E - (E-1)H}{E}\right) - (E+1)\ln(1-H) \quad (7)$$

A, B and E being fitted constants that are characteristic of each material. In this model, θ is interpreted as the fraction of the polymer surface covered by at least one layer of water molecules; $A\theta$ as the mass of water in a complete monolayer, expressed (like all masses in the model) as a fraction of the dry mass of the polymer; $A(\theta + \beta)$ as the externally adsorbed moisture (so that $A\beta$ is the mass of water which is adsorbed beyond the mass of the monolayer); B as the mass of water absorbed internally at 1.0 relative humidity; $B\theta H$ as the mass of internally absorbed water when the monolayer coverage is θ and the relative humidity H; and E as a kind of equilibrium constant (though without regard to entropy effects) between monolayer water and the 'normally condensed' water adsorbed externally to the monolayer

$$E = \exp[-(q_l - q_L)/(k_B T)] \quad (8)$$

where q_L (J mol^{-1}) is the heat of condensation of water, q_l (J mol^{-1}) is the heat of adsorption of water on the polymer, T (K) is the temperature and k_B is the Boltzmann constant (1.38×10^{-23} J K^{-1}).

To apply the GAB model

$$W = C_g K W_m [Pr^{-1} + (C_g - 2)K + (1 - C_g)K^2 P_r]^{-1} \quad (9)$$

where W is the weight (g) of sorbed water per gram of polymer, W_m is the weight (g) of water in a complete monolayer per gram of polymer, C_g and K are constants related to the heat of sorption and P_r is the relative pressure of water vapour [36], W_m, C_g and K were optimized using a linear model to determine the regression of P_r/W on P_r and P_r^2 [15,36].

2.2.6. Enthalpy of hydration/dissolution

The enthalpies of interaction between bulk liquid water and 0.05–0.1 g hydroxypropylcellulose samples with various pre-established moisture contents were determined in duplicate using a Tronac 458 isoperibol microcalorimeter and Tronac FS101 calorimetry software. To eliminate differences due to differences in particle size, HPC samples comprised only particles with diameters <250 μm. The enthalpy released per min by each polymer was calculated as the quotient of the enthalpy measured using the dry sample and the time taken for its complete reaction [37].

2.2.7. Non-freezing water

Known masses of dry polymer in 6 mm aluminium crucibles were treated with known masses of distilled water, and the crucibles were sealed and stored at 20°C for 48 h. Differential scanning calorimetry was then performed in a Shimadzu DSC-50 apparatus [3], the samples being first cooled to -30°C at 5 K min^{-1}, and then heated to 30°C at 5 K min^{-1}; enthalpies of melting were determined by integration of the melting peaks [38]. The capacity of the polymers to bind water strongly in non-freezing form ('water-binding capacity') was estimated by regressing melting enthalpy on the mass of water in the system and extrapolating to zero melting enthalpy [39]. The same DSC protocol was used to screen for freezing water in polymer samples stored at the relative humidities specified in Section 2.2.5. To refer the amount of non-freezing water to each polymer repeat unit, the mean molecular weight of the repeat unit of each polymer was calculated by structural considerations from the mean values of DS and MS estimated by ^{13}C NMR; the number of molecules of non-freezing water per repeat unit was calculated by dividing the mass of non-freezing water per 100 g of polymer by the molecular weight of water and by the number of moles of repeat unit corresponding to 100 g of polymer [3].

2.2.8. Rate of water uptake by compacts

The rate of water uptake by 10 mg polymer compacts (prepared in an Erweka Korsch-Eko excentric tablet press using 6 mm flat punches and a compression force of 2600 N) was determined in duplicate by differential scanning calorimetry in a Shimadzu DSC-50 apparatus [3,39]. Each tablet was placed in an aluminium sample holder, 15 mg of distilled water was added, and after 5, 10, 15, 30 or 60 min (for L-HPCs) or 5, 15, 30, 60 or 240 min (for HPCs), non-freezing water (identified with water uptake) was calculated from the melting enthalpy determined as described above. Following Wan et al. [24], the resulting water uptake profiles were fitted with the biexponential equation

$$U = k_1 t^{0.1} + k_2 t^{0.5} \quad (10)$$

where U is the water uptake achieved by time t, expressed as a percentage of the total mass of the polymer + water system, and k_1 and k_2 are kinetic constants related to the mechanism of water uptake (capillarity-driven and diffusive, respectively).

2.2.9. Statistical analysis

The influence of the characteristics of the L-HPCs and HPCs on the parameters characterizing water–polymer interaction was evaluated by stepwise multiple linear regression using Statgraphics® v. 7.0 with a significance level α of 0.05. Goodness of fit was assessed by analysis of variance of the regression [40].

3. Results and discussion

3.1. Structural and physical characteristics of the polymers

^{13}C NMR spectroscopy was chosen for characterization of the substituent contents of the polymers because it allows quantification of substitution at each substitutable glucopyranose hydroxyl as well as of total substituent content [31,32,41]. It showed (Table 1) that in the L-HPCs studied, all the hydroxypropyl groups are attached via glucopyranose position 6 (to within experimental error) and all or almost all substituent side chains are just one hydroxypropyl group long (the MS and total DS values are identical except for a small difference in the case of LH-20). All the HPCs studied have very similar position-specific and total DS values; in all of them, substitution is significantly more intense at positions 2 and 6 than at position 3, and the average substituent length (MS/DS ratio) is about 1.6 hydroxypropyl groups (rather longer in the Klucel® than in the Nisso® varieties).

The HPCs proved to be fundamentally amorphous, with crystallinity index values of about 0.4, well below the range 0.62–0.86 typical of MCCs [42], although the Klucel® varieties are slightly more crystalline than the others (Table 1). The L-HPCs have crystallinities spanning the whole range between those of the HPCs and those of MCCs.

L-HPC particles are very much smaller than HPC particles, and Nisso® HPCs are much smaller than Klucel® HPCs (Table 1). L-HPCs all have greater specific area (Table 1), and larger total pore volume and smaller mean pore diameter (Fig. 1), than any HPC, although within each group both specific surface area and pore size distribution vary considerably from one variety to another (in particular, among the HPCs the Nisso® varieties have significantly larger pore volumes (between 0.460×10^{-3} and 0.543×10^{-3} cm^3 g^{-1}) than the Klucel® varieties (between 0.371×10^{-3} and 0.437×10^{-3} cm^3 g^{-1})).

Table 1
Some molecular and structural characteristics of the hydroxypropylcelluloses studied[a]

Polymer	DS2/DS3/DS6[b]	DS_t[c]	Molar substitution	% HPO[d]	Crystallinity	Martin diameter (μm)	Specific surface area ($m^2\ g^{-1}$)
LH-11	–/–/0.26	0.26	0.26	10.9 (0.3)	0.51	32.5 (2.2)	1.10 (0.05)
LH-20	–/–/0.30	0.30	0.33	13.5 (0.2)	0.43	25.5 (2.4)	0.77 (0.01)
LH-21	–/–/0.25	0.25	0.25	10.6 (0.1)	0.60	22.0 (2.1)	1.22 (0.01)
LH-22	–/–/0.18	0.18	0.18	7.6 (0.2)	0.69	23.9 (2.4)	0.99 (0.06)
LH-31	–/–/0.26	0.26	0.26	10.9 (0.3)	0.46	13.9 (1.9)	2.20 (0.02)
Klucel®GF	0.9/0.5/0.9	2.3	3.86	64.5 (0.1)	0.44	286.1 (1.9)	0.26 (0.01)
Nisso®MBJ	0.9/0.5/0.8	2.2	3.48	62.1 (0.1)	0.39	142.8 (1.5)	0.31 (0.01)
Nisso®MDC	0.9/0.5/0.8	2.2	3.56	62.7 (0.1)	0.39	132.3 (1.6)	0.32 (0.02)
Nisso®MJD	0.9/0.5/0.8	2.2	3.37	61.4 (0.1)	0.38	149.7 (1.6)	0.29 (0.01)
Nisso®HBJ	0.9/0.5/0.9	2.3	3.42	61.7 (0.1)	0.40	136.3 (1.6)	0.31 (0.03)
Nisso®HJE	0.9/0.5/0.8	2.2	3.44	61.9 (0.1)	0.38	143.1 (1.6)	0.29 (0.01)
Klucel®MF	0.9/0.6/0.9	2.4	3.89	64.7 (0.1)	0.44	245.2 (2.0)	0.26 (0.02)

[a] In parenthesis, SD.
[b] Degrees of substitution at anhydroglucose positions 2, 3 and 6.
[c] Total degree of substitution.
[d] Hydroxypropyloxy content.

3.2. Interaction with water vapour

Hydroxypropylcellulose samples exposed to various relative humidities showed no DSC melting transitions. All the water sorbed under these conditions is therefore bound to the hydrophilic groups of the polymer. However, since DSC provided no information on the topological distribution of the water in these samples, the fraction of moisture present in different zones of the hydroxypropylcellulose particles were estimated by fitting Young–Nelson [4] and GAB [36] equations to the experimental moisture sorption–desorption data. Fig. 2 shows the sorption–desorption isotherms of a typical L-HPC (LH-11) and a typical HPC (Klucel® MF). Like those of HPMCs [12], both are Brunauer Type III isotherms, whereas those of MCCs are of Type II [7]. Although Type III isotherms have been thought to be associated with systems in which the heat of adsorption is less than the heat of condensation of the adsorbate, the estimated values of the parameter E of the Young–Nelson model (Table 2) suggest that this is not the case for L-HPCs, for which $E < 1$ (for the interpretation of the Young–Nelson parameters, see Section 2.2.5).

All the Young–Nelson parameters listed in Table 2 are of the same order of magnitude as those reported for several varieties of HPMC by Malamataris et al. [15] and Nokhodchi et al. [12]. The parameter E is in all cases significantly larger than for MCC [36], whose greater crystallinity must result in a greater heat of adsorption. The fact that the L-HPCs all have smaller E values than the HPCs (Table 2) likewise implies that monolayer water is bound more strongly to LHPCs than to HPCs, which is again in consonance with the greater crystallinity and smaller degree of substitution of L-HPCs (Table 1).

The values of the Young–Nelson parameter A listed in Table 2 show that L-HPCs have a smaller capacity for adsorption of water vapour than HPCs (about 0.2–0.3 molecules of water per L-HPC repeat unit, as against about 0.9–1.0 for HPCs), while the values of B show them to have a greater capacity for internal absorption. The former difference may probably be attributed to the lower degree of substitution of L-HPCs, and the latter to their larger pore volumes (Fig. 1). The influence of the degree of substitution on the capacity for monolayer adsorption may be attributed to the tendency of water molecules to interact with hydrophilic groups [28,38]. It is also seen in the finding that among HPMCs adsorption capacity increases with the hydroxypropyl/methyl ratio [15,16]. Note that it is the degree of substitution, rather than the molar substitution, that determines the adsorption capacity (probably because the addition of a further hydroxypropyl unit to one that is already present does not change the number of terminal hydroxyl groups). The adsorption capacities of the HPCs with the greatest molar substitution

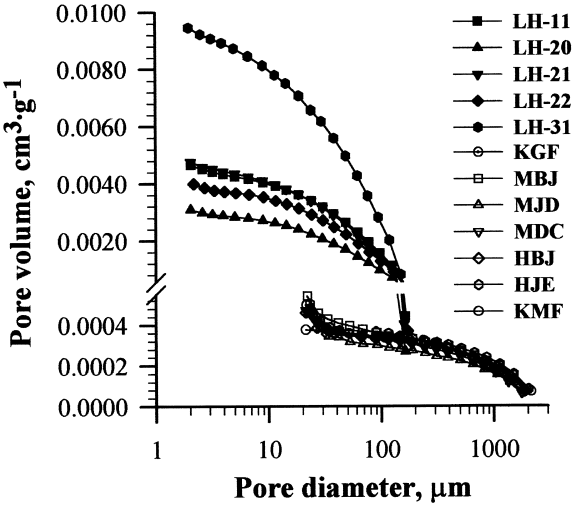

Fig. 1. Plots of cumulative pore volume against pore diameter, for the hydropropylcelluloses studied.

values (the Klucel® products) are no greater than those of the other HPCs.

The differences in A and B among the various hydroxypropylcelluloses are reflected in Table 3, which for each of them lists the adsorbed monolayer water contents $A\theta$, total adsorbed water contents $A(\theta + \beta)$ and absorbed water contents $B\theta H$, as predicted by the Young–Nelson model for each of the relative humidity conditions employed. For both kinds of hydroxypropylcellulose, the values of A, $A\theta$ and $A(\theta + \beta)$ imply that for any given relative humidity, the amount of water adsorbed beyond the mass of the monolayer water is virtually the same multiple of the amount in a complete monolayer; for example, at a relative humidity of 0.939, $\beta = 3.5$–3.6 for L-HPCs and 3.7–3.8 for HPCs.

To explore further the factors influencing adsorption and absorption of water vapour, stepwise multiple regression analysis was performed to determine the dependence of $A\theta$, $A(\theta + \beta)$ and $B\theta H$ on the polymer characteristics at a relative humidity of 0.939. The initial independent variable set included the particle diameter, specific surface area, pore volume, pore diameter, DS, MS and hydroxypropyl group content; and because of the clear division of the hydroxypropylcelluloses in two groups closely, which are clustered about just two hydroxypropyl content values, this latter variable was constrained to enter the regression equation only to first order. The results of stepwise polynomial regression analysis (3 and 9 degrees of freedom, $\alpha < 0.01$) are as follows

$$A\theta = 0.3225 \times \%\mathrm{HPO} - 0.0563 \times D_p + 4.9 \times 10^{-5} \times D_p^2;\ r^2 = 0.9886 \quad (11)$$

$$A(\theta+\beta) = 1.5052 \times \%\mathrm{HPO} - 0.2530 \times D_p + 2.2 \times 10^{-4} \times D_p^2;\ r^2 = 0.9896 \quad (12)$$

$$B\theta H = 4.6469 \times V_p - 0.3217 \times V_p^2 + 1.5 \times 10^{-5} \times D_p^2;\ r^2 = 0.9508 \quad (13)$$

where *%HPO* is the hydroxypropyloxy content (% of dry mass), D_p is pore diameter (nm), and V_p is pore volume (ml g^{-1}). These equations show that both monolayer water content and total adsorbed water content increased with increasing hydroxypropyl content and decreased with increasing mean pore diameter, while internally absorbed water increased with both mean pore diameter and pore volume. These dependences support the applicability of the Young–Nelson model, in which the absorbed water is water that has diffused through pores into the core of the particle from the adsorbed monolayer, and the monolayer water is therefore the result of the balance between surface binding forces and diffusion forces [12]. It is possible that the failure to take the particle microstructure into account may have been responsible for the discrepancies among the studies of HPMCs that have attempted to explain the variation in the adsorption/absorption ratio in terms of particle size [12,15].

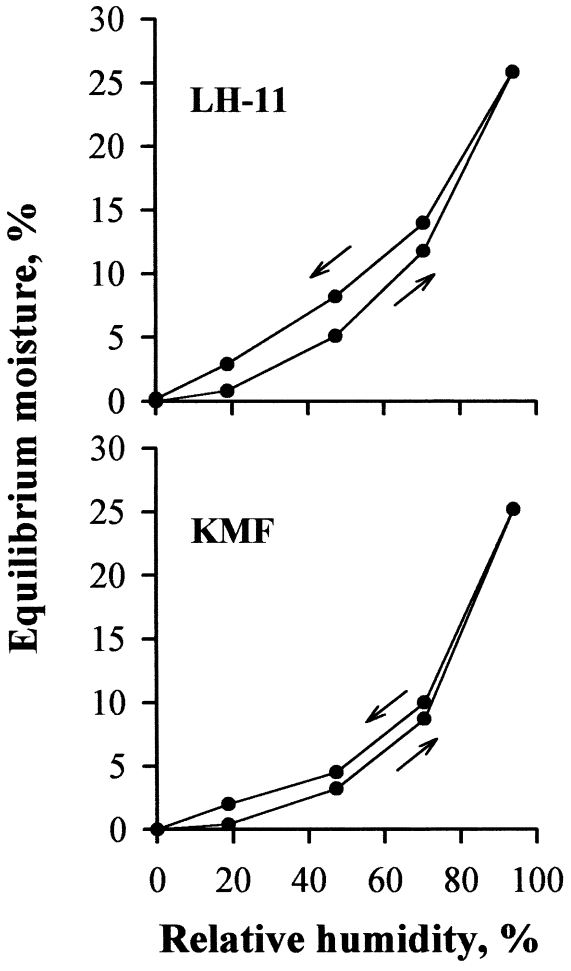

Fig. 2. Sorption–desorption isotherms of the L-HPC LH-11 and the HPC Klucel® MF.

Table 2
Optimized values of the parameters of Young and Nelson's [4] model of uptake of water vapour

Polymer	E	A	B	r^2	F value[a]
LH-11	0.82	0.033	0.126	0.9930	987.2
LH-20	0.78	0.033	0.132	0.9941	1184.1
LH-21	0.78	0.034	0.130	0.9924	911.4
LH-22	0.78	0.019	0.203	0.9924	526.1
LH-31	0.78	0.020	0.181	0.9915	814.2
Klucel®GF	1.2	0.046	0.068	0.9967	2129.7
Nisso®MBJ	1.2	0.044	0.079	0.9944	1233.5
Nisso®MDC	1.2	0.043	0.080	0.9963	1873.2
Nisso®MJD	1.2	0.047	0.062	0.9982	3841.9
Nisso®HBJ	1.2	0.050	0.060	0.9911	775.8
Nisso®HJE	1.2	0.051	0.036	0.9990	7175.6
Klucel®MF	1.2	0.045	0.047	0.9975	2753.1

[a] Two and 13 degrees of freedom; $\alpha < 0.01$.

Table 3
Monolayer water $A\theta$, total adsorbed water $A(\theta + \beta)$ and absorbed water $B\theta H$ in hydroxypropylcelluloses stored at various relative humidities H (% of dry mass of hydroxypropylcellulose)

Polymer	0.188 H			0.472 H			0.704 H			0.939 H		
	$A\theta$	$A(\theta+\beta)$	$B\theta H$	$A\theta$	$A(\theta+\beta)$	$B\theta H$	$A\theta$	$A(\theta+\beta)$	$B\theta H$	$A\theta$	$A(\theta+\beta)$	$B\theta H$
LH-11	0.7	0.7	0.5	1.7	2.0	3.1	2.4	5.2	6.6	3.1	14.8	11.2
LH-20	0.7	0.7	0.6	1.8	2.1	3.3	2.5	5.4	7.0	3.2	15.0	11.8
LH-21	0.8	0.8	0.6	1.8	2.1	3.3	2.5	5.5	6.9	3.3	15.2	11.6
LH-22	0.4	0.4	0.9	1.0	1.2	5.1	1.4	3.0	10.8	1.8	8.5	18.1
LH-31	0.4	0.4	0.8	1.1	1.2	4.5	1.5	3.2	9.6	1.9	9.0	16.1
Klucel®GF	0.7	0.7	0.2	2.0	2.3	1.3	3.0	6.7	3.1	4.3	21.5	5.8
Nisso®MBJ	0.7	0.7	0.2	1.9	2.2	1.6	2.9	6.4	3.7	4.1	20.6	6.9
Nisso®MDC	0.7	0.7	0.2	1.8	2.2	1.6	2.8	6.2	3.7	4.0	20.1	7.0
Nisso®MJD	0.7	0.7	0.2	2.0	2.4	1.2	3.1	6.8	2.9	4.4	22.0	5.4
Nisso®HBJ	0.8	0.7	0.2	2.1	2.5	1.2	3.3	7.2	2.8	4.6	23.4	5.2
Nisso®HJE	0.8	0.7	0.1	2.2	2.6	0.7	3.4	7.4	1.7	4.7	23.9	3.2
Klucel®MF	0.7	0.7	0.1	1.9	2.3	0.9	3.0	6.5	2.2	4.2	21.1	4.1

To judge by the r^2 columns of Tables 2 and 4, the GAB model (Table 4) fits the data less well than the Young–Nelson model, possibly because the sharp rise in water uptake at relative humidities greater than about 0.70 may be incompatible with the GAB assumption that adsorption is restricted to the particle surface [12,36]. This may also explain why, according to the GAB model, L-HPCs adsorb more monolayer water than HPCs. Interestingly, expressing the GAB figures for monolayer water in terms of the number of molecules of water per polymer repeat unit gives values of about 0.3–0.4 for L-HPCs and 0.7–0.8 for HPCs. These are quite similar to the values estimated using the more comprehensive Young–Nelson model.

3.3. Hydration/dissolution

For all the hydroxypropylcelluloses, hydration/dissolution is an exothermic process, as in the case of other cellulose ethers [3]. Although the enthalpies of interaction of HPCs are more negative than those of L-HPCs (Table 5), it must be borne in mind that HPCs are soluble and L-HPCs are not; thus, whereas the measured enthalpies of the HPCs are the balance of all the processes involved in dissolution – hydration, replacement of intermolecular bonds by interactions with water, conformational changes, etc. [3,43] – those of the L-HPCs are just the enthalpies of hydration of the undissolved particles. In fact, for L-HPCs the presence of bulk water adds only about 25% to the enthalpy of hydration by water vapour, estimated as the difference between the measured enthalpies of hydration of the dry hydroxypropylcellulose and hydroxypropylcellulose stored for 6 months at a relative humidity of 0.939 (Table 5); and the DSC-measured water-binding capacities of the L-HPCs (Table 6) are similarly only an average 20% greater than their water vapour uptake at 0.939 relative humidity (Fig. 2, Table 3).

The insolubility of the L-HPCs can be attributed to their relatively high crystallinity and low degree of substitution: high crystallinity generally implies that a large amount of energy is required to break the bonds responsible for the crystalline solid state [43,44], while the replacement of hydroxyl groups by ether groups reduces the number of intermolecular polymer–polymer hydrogen bonds [30]. In spite of their insolubility, the absolute values of the enthalpies of hydration of the L-HPCs are nevertheless remarkably high, about 70 J g^{-1} as against 10 J g^{-1} for ethylcellulose (EC) [3] and 35–50 J g^{-1} for MCC [41], both of which, like the L-HPCs, are insoluble. Whereas the low value of EC in comparison with MCC is attributed to a reduction in the number of hydroxyl groups available for the formation of hydrogen bonds with water, the high values of the L-HPCs can be attributed to their hydroxypropyl groups providing hydroxyl groups that are more available to solvation by water molecules than those of MCC.

Table 4
Optimized values of the parameters of the GAB model of uptake of water vapour

Polymer	W_m (%)	C_g	K	r^2	F value[a]
LH-11	3.96	44.65	0.918	0.9082	70.2
LH-20	4.15	31.11	0.919	0.8152	31.9
LH-21	4.29	36.06	0.910	0.8574	43.1
LH-22	3.47	37.40	0.876	0.8677	46.9
LH-31	3.33	31.58	0.900	0.8190	32.6
Klucel®GF	2.79	46.04	0.967	0.9155	76.9
Nisso®MBJ	2.83	48.37	0.968	0.9224	84.2
Nisso®MDC	2.83	46.56	0.966	0.9166	77.9
Nisso®MJD	2.81	47.36	0.968	0.9182	79.5
Nisso®HBJ	2.74	51.44	0.974	0.9329	98.3
Nisso®HJE	2.78	50.09	0.966	0.9242	86.3
Klucel®MF	2.64	60.89	0.962	0.9490	131.3

[a] Two and 12 degrees of freedom; $\alpha < 0.01$.

Table 5
Enthalpies of interaction between hydroxypropylcelluloses and bulk water, with the corresponding reaction times, and energy released by hydroxypropylcelluloses upon sorption of water vapour at a relative humidity of 0.939 (in parentheses, SD)

Polymer	Enthalpy of interaction ($J\ g^{-1}$)	Reaction time (s)	Enthalpy released per min ($J{\cdot}g^{-1}{\cdot}min^{-1}$)	Sorption energy ($J{\cdot}g^{-1}$)
LH-11	−70.92 (1.88)	65 (2)	65.46	57.65 (0.68)
LH-20	−69.97 (2.90)	60 (2)	69.97	55.26 (0.47)
LH-21	−69.95 (2.71)	63 (2)	66.62	56.33 (0.77)
LH-22	−62.86 (0.30)	60 (2)	62.86	51.91 (0.11)
LH-31	−71.35 (0.17)	63 (2)	67.95	57.15 (0.17)
Klucel®GF	−83.84 (1.87)	320 (6)	15.72	37.62 (0.63)
Nisso®MBJ	−96.16 (0.38)	242 (10)	23.84	46.16 (0.10)
Nisso®MDC	−97.11 (1.34)	253 (13)	23.03	47.45 (0.20)
Nisso®MJD	−98.08 (0.23)	241 (12)	24.42	49.64 (0.98)
Nisso®HBJ	−97.69 (1.23)	224 (2)	26.17	45.48 (1.80)
Nisso®HJE	−99.80 (0.85)	227 (4)	26.38	48.98 (1.53)
Klucel®MF	−82.95 (0.54)	330 (2)	15.08	35.98 (0.85)

This interpretation is supported by the fact that the L-HPC with the smallest enthalpy of hydration, LH22, is the one with the lowest degree of substitution. Note, also, that according to the DSC results, even the L-HPC with the smallest water-binding capacity (again LH-22) binds considerably more non-freezing water than EC, the substituents of which have no hydroxyl groups: 2.65 molecules per repeat unit (Table 6) as against 1.6 for EC [15].

The solubility of the HPCs is doubtless facilitated by their high degrees of substitution and low crystallinity. Due to their solubility, their reaction with water takes longer (see reaction times, Table 5) and is not complete unless at least 1.5 times their weight of water is present, as against only about 0.6 for L-HPCs (Fig. 3). The enthalpies of dissolution of the Nisso® varieties are very similar to those of the HPMC Methocel® E5 (100.4 J g^{-1}) [3], whereas those of the Klucel® varieties are about 15 J g^{-1} lower, either because of their smaller specific surface areas [37] – although the exclusion of particles with diameters >250 μm must have limited this effect – or because of their greater crystallinity, which implies greater expenditure of energy in the disruption of polymer–polymer interactions [44] (Table 1). The slightly greater MS values of the Klucel® varieties may also play a role, since they increase molecular weight without increasing the number of terminal hydroxyl groups. These findings are reflected in Fig. 4, which shows the results of a statistical analysis of the influence of molar substitution and crystallinity on the enthalpies of dissolution of the HPCs.

The states of water in homogeneous mixtures of water and amorphous polymers are the subject of current debate [11,45]. DSC methods have been used extensively to determine the minimum amount of water needed for full hydration of cellulose ethers [8,11], a parameter that can affect the rheological [6] and transport properties [46] of the polymer

Table 6
Capacities of hydroxypropylcelluloses to bind non-freezing water, as determined by differential scanning calorimetry (in parentheses, SD)

Polymer	Water-binding capacity (% of dry mass of hydroxypropylcellulose)	Molecules H_2O/ Polymer repeat unit
LH-11	31.13 (2.27)	3.06 (0.08)
LH-20	36.78 (1.20)	3.93 (0.15)
LH-21	35.30 (1.70)	3.46 (0.15)
LH-22	27.68 (2.04)	2.65 (0.19)
LH-31	42.47 (1.61)	4.19 (0.17)
Klucel®GF	79.60 (2.11)	18.10 (0.33)
Nisso®MBJ	94.17 (2.08)	21.36 (0.29)
Nisso®MDC	94.25 (1.96)	21.37 (0.23)
Nisso®MJD	92.75 (0.95)	21.07 (0.17)
Nisso®HBJ	98.69 (3.09)	22.42 (0.68)
Nisso®HJE	96.89 (3.68)	22.01 (0.60)
Klucel®MF	87.06 (3.38)	19.77 (0.89)

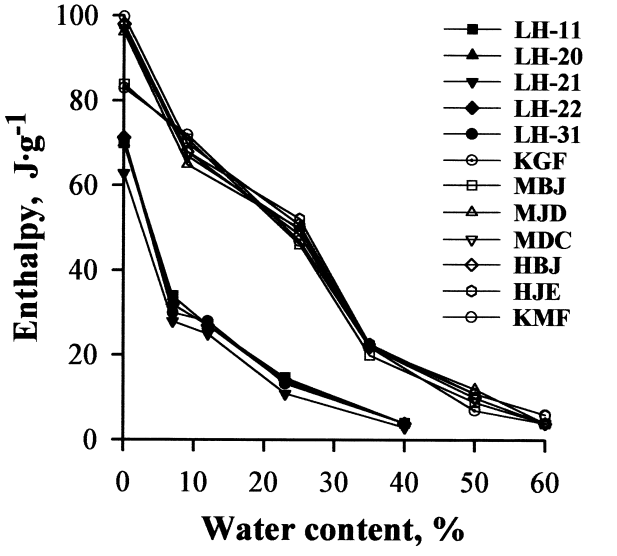

Fig. 3. Enthalpies of interaction between bulk water and hydroxypropylcellulose samples with various pre-existing water contents.

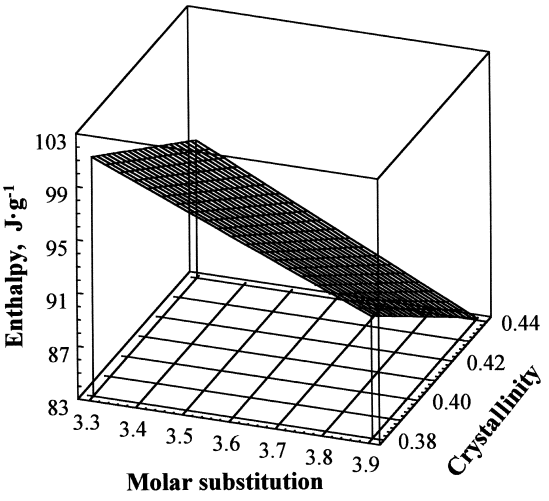

Fig. 4. Dependence of the enthalpy of dissolution of HPCs on their molar substitution and crystallinity.

gel and also the stability of any other component of such systems [18,47]. In those studies, the amount of water needed for full hydration is identified with the amount of non-freezing water, which can be determined regardless of whether, as in this work and many other studies of cellulose ethers [38], the DSC scans exhibit just a single crystallization/melting transition instead of two (one for free water and one for freezing bound water). Since the time taken for the DSC signal to return to baseline following the onset of crystallization, less than 30 s, suggests that temperature was decreased slowly enough to allow all freezable water to freeze [9], this single peak is assumed to represent both free water and any freezing bound water (the DSC signal for which is presumably masked by the tail of the signal for free water). The non-freezing water content, which is not represented in the crystallization and melting peaks, is determined as described in Section 2.2.4. The results (Table 6) show that all the HPCs bind about three times more molecules of non-freezing water per repeat unit than the 6.2 reported by Joshi and Wilson [3] for Methocel® E5, a variety of HPMC which has lower hydroxyl and hydroxypropyl contents. Among the HPCs, most of the Nisso® varieties bind just a molecule or so more water per repeat unit than the Klucel® varieties, but because of the greater molar substitution of the latter there is a rather larger difference in water-binding capacity on a dry weight basis: 80–87% for the Klucel® varieties as against 93–99% for the Nisso® varieties.

3.4. Water uptake by hydroxypropylcellulose compacts

Some important industrial applications of cellulose ethers use the polymer in compacted form [8,26]. The utility of the compacts depends on the way they take up water which depends on the structural properties of the polymer and can provide useful information about these properties [48].

In this work, 10 mg L-HPC compacts took just 5 min or so to take up all the water they could (rapidly swelling and disintegrating in the process), but HPC compacts took over 1 h (Fig. 5). This difference is in agreement with the much faster reaction of L-HPCs in powder form (Table 5), which can be attributed both to their much smaller particle size and, in particular, to their insolubility, because of which the interactions in which L-HPCs are involved are much less complex than those of HPCs.

When water penetrates solid hydroxypropylcellulose, it inserts itself into the hydrogen-bonded links between adjacent polymer chains which become more and more independent of each other, as more and more water comes between them. As the individual chains gain rotational freedom, they occupy more space, which results in the swelling of the polymer mass. The penetrating water fills the voids between the polymer chains and diffuses into denser regions of the polymer, forcing additional chains apart. The Wan et al. [24] model of water uptake kinetics, Eq. (10), considers two water uptake mechanisms: capillarity-driven uptake through interparticle porous (associated with the constant k_1) and diffusive uptake through the swollen polymer (associated with k_2). This two-mechanism model is supported by recent studies of the mobility of water in hydrophilic polymer systems, which have found evidence for two states of water [45,48,49]. The water molecules close to the polymer

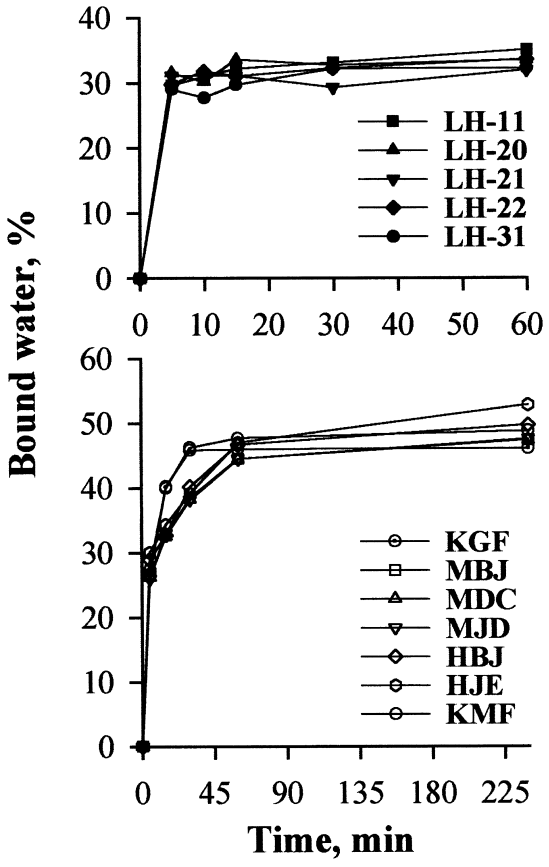

Fig. 5. Kinetics of uptake of non-freezing water hydroxypropylcellulose compacts.

Table 7
Results of fitting the Wan et al. [24] model to the kinetics of water uptake by HPC tablets

Polymer	k_1 ($min^{-0.1}$)[a]	k_2 ($min^{-0.5}$)[a]	r^2	F value[b]
Klucel®GF	30.18	0.02	0.9450	470.0
Nisso®MBJ	24.22	0.49	0.9720	884.6
Nisso®MDC	24.30	0.47	0.9757	1027.1
Nisso®MJD	24.25	0.49	0.9745	972.1
Nisso®HBJ	25.52	0.48	0.9740	962.1
Nisso®HJE	25.28	0.57	0.9869	1900.0
Klucel®MF	29.53	0.01	0.9363	392.8

[a] k_1 and k_2 are the coefficients of Eq. (10).
[b] Two and 10 degrees of freedom; $\alpha < 0.01$.

reorient more slowly than the water molecules in contact with other water molecules, which indicates that they are located in a highly restrictive environment and suggests that strong interaction occurs between the sorbed water and the polymer. Klucel® HPCs differ significantly from the Nisso® varieties as regards the relative importance of the two mechanisms in the Wan et al. model: capillarity-driven uptake predominates in all the HPCs, but whereas diffusive uptake eventually acquires importance for the Nisso® varieties, it remains negligible for the Klucel® varieties (Table 7). Regression analysis (Fig. 6) suggests that the slightly larger k_1 values and the very much smaller k_2 values of the Klucel® varieties are due to their larger particle size and greater molar substitution, larger particle size implying larger interparticle pores and easier capillary uptake [39] and greater molar substitution implying a somewhat smaller water-binding capacity (Table 6). The influence of particle size was confirmed by the results of experiments on compacts prepared from the 105–200 μm fraction of Klucel® MF; this reduction in particle size reduced k_1 from 29.53 to 24.92 and increased k_2 from 0.01 to 0.29 ($r^2 = 0.9686$).

4. Conclusions

The moisture sorption and desorption profiles of the various hydroxypropylcelluloses studied were fitted better by the Young–Nelson model than by the GAB models. This implies that the water vapour is not merely adsorbed onto the particle surface, but is also adsorbed into the interior of the polymer particle. The optimized values of the Young–Nelson parameter E are interpreted as showing that the binding energy of the first external monolayer of water is greater for L-HPCs than for HPCs, and this is attributed to the greater crystallinity and smaller degree of substitution of the former. In comparison with HPCs, L-HPCs also have smaller values of the Young–Nelson parameter A, which is related to the amount of the water in a complete external monolayer, and larger values of the parameter B, which is related to the amount of absorbed water; the difference in A is attributed to the lower substituent contents of L-HPCs, and the difference in B to the greater porosity of their particles.

The finding that the hydration process of L-HPCs is less exothermic and terminates sooner than the hydration/dissolution process of HPCs is likewise attributed to the greater crystallinity and lower substituent content of the former, since these differences lead to L-HPCs being less soluble and having a smaller capacity to bind non-freezing water than HPCs.

Finally, L-HPC compacts differ significantly from HPC compacts as regards the rate at which they take up water and the relative importance of the mechanisms by which this occurs. In the case of L-HPCs, water uptake is rapid and leads to the disintegration of the compact, whereas HPC compacts take up more water, more slowly. Furthermore, the water uptake profiles of HPCs with small particles and relatively low molar substitution reflect both rapid initial capillarity-driven uptake through pores in the polymer particles, and slower subsequent diffusion through the hydrated polymer; in contrast, HPCs with larger particles and higher molar substitution only undergo capillarity-driven water uptake.

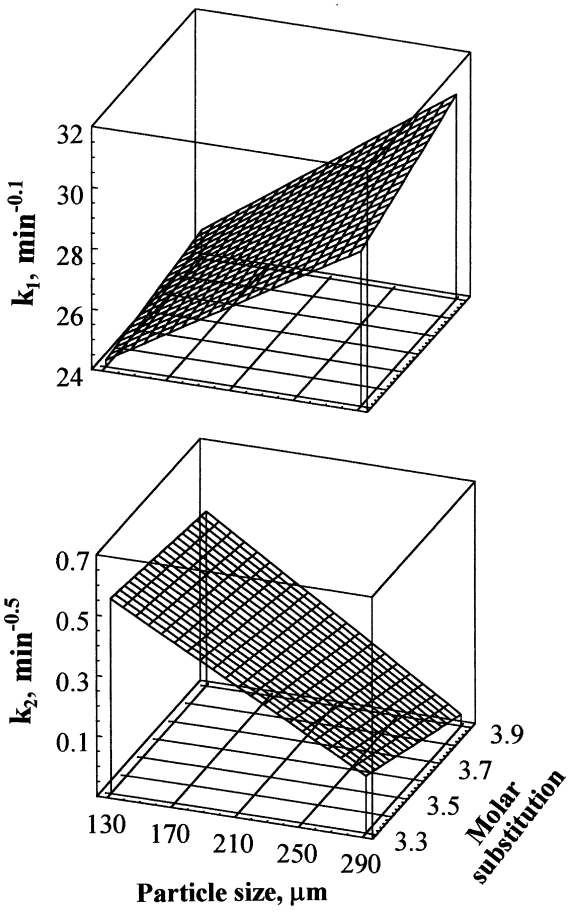

Fig. 6. Dependence of k_1 and k_2, Eq. (10), on HPC particle size and molar substitution.

Acknowledgements

This work was supported by the Spanish Ministry of Education and Science under CICYT project SAF96-1706. We thank the Xunta de Galicia for an equipment grant (DOG 04/06/97), and Shin-Etsu Chemical (Japan), Nippon Soda (Japan) and Aqualon (USA) for generous gifts of L-HPC and HPC samples.

References

[1] G. Zografi, States of water associated with solids, Drug Dev. Ind. Pharm. 14 (1988) 1905–1926.
[2] B.C. Hancock, S.L. Shamblin, Water vapour sorption by pharmaceutical sugars, Phatm. Sci. Technol. To. 1 (1998) 345–351.
[3] H.N. Joshi, T.D. Wilson, Calorimetric studies of dissolution of hydroxypropyl methylcellulose E5 (HPMC E5) in water, J. Pharm. Sci. 82 (1992) 1033–1038.
[4] J.H. Young, G.H. Nelson, Theory of hysteresis between sorption and desorption isotherms in biological materials, Trans. Am. Soc. Agric. Eng. 10 (1967) 260–263.
[5] C.J. Roberts, F. Franks, Crystalline and amorphous phases in the binary system water-β,β-trehalose, J. Chem. Soc. Faraday Trans. 92 (1996) 1337–1343.
[6] R. Tanaka, T. Hatakeyama, H. Hatakeyama, Differential scanning calorimetry studies on water restrained in hydroxyethylcellulose and hydrophobically modified hydroxyethylcellulose, Macromol. Chem. Phys. 198 (1997) 883–898.
[7] G.R. Sadeghnejad, P. York, N.G. Stanley-Wood, Water vapour interaction with pharmaceutical cellulose powders, Drug Dev. Ind. Pharm. 12 (1986) 2171–2192.
[8] Y. Kawashima, H. Takeuchi, T. Hino, T. Niwa, T.L. Lin, F. Sekigawa, M. Ohia, The effects of particle size, degree of hydroxypropyl substitution and moisture content of low-substituted hydroxypropylcellulose on the compactability of acetominophen and the drug release rate of the resultant tablets, S.T.P. Pharma. Sci. 3 (1993) 170–177.
[9] G. Sartor, G.P. Johari, Thermodynamic equilibrium of water and ice in hydrated gliadin and hemoglobin, J. Phys. Chem. B 101 (1997) 6575–6582.
[10] G.P. Johari, Thermodynamics of water-cubic ice and other liquid-solid coexistence in nanometer-size particles, J. Chem. Phys. 109 (1998) 1070–1073.
[11] C.B. McCrystal, J.L. Ford, A.R. Rajabi-Siahboomi, A study on the interaction of water and cellulose ethers using differential scanning calorimetry, Thermochim. Acta 294 (1997) 91–98.
[12] A. Nokhodchi, J.L. Ford, H.M. Rubinstein, Studies on the interaction between water and (hydroxypropyl)methylcellulose, J. Pharm. Sci. 86 (1997) 608–615.
[13] B.C. Hancock, G. Zografi, The relationship between the glass transition temperature and the water content of amorphous pharmaceutical solids, J. Pharm. Sci. 86 (1997) 1–12.
[14] F. Franks, Phase changes and chemical reactions in solid aqueous solutions: science and technology, Pure Appl. Chem. 69 (1997) 915–920.
[15] S. Malamataris, T. Karidas, P. Goidas, Effect of particle size and sorbed moisture on the compression behaviour of some hydroxypropyl methylcellulose (HPMC) polymers, Int. J. Pharm. 103 (1994) 205–215.
[16] S. Malamataris, T. Karidas, Effect of particle size and sorbed moisture on the tensile strength of some tableted hydroxypropyl methylcellulose (HPMC) polymers, Int. J. Pharm. 104 (1994) 115–123.
[17] A. Nokhodchi, J.L. Ford, H.P. Rowe, H.M. Rubinstein, The influence of moisture content on the consolidation properties of hydroxypropylmethylcellulose K4M (HPMC 2208), J. Pharm. Pharmacol. 48 (1996) 1116–1121.
[18] C. Alvarez-Lorenzo, J.L. Gómez-Amoza, R. Martínez-Pacheco, C. Souto, A. Concheiro, The stability of theophylline with a hydroxypropylcellulose matrix, Drug Dev. Ind. Pharm. 26 (2000) 13–20.
[19] S. Otsuki, K. Adachi, T. Taguchi, novel fibre-optic gas-sensing configuration using extremely curved optical fibers and an attempt for optical humidity detection, Sensor Actuat. B-Chem. 53 (1998) 91–96.
[20] R. Duro, C. Alvarez, R. Martínez-Pacheco, J.L. Gómez-Amoza, A. Concheiro, C. Souto, The adsorption of cellulose ethers in aqueous suspensions of pyrantel pamoate: effects on zeta potential and stability, Eur. J. Pharm. Biopharm. 45 (1998) 181–188.
[21] R. Duro, C. Souto, J.L. Gómez-Amoza, R. Martínez-Pacheco, A. Concheiro, Cellulose ethers-polysorbate 80 interactions. Implications on the stability of pyrantel pamoate suspensions, Chem. Pharm. Bull. 46 (1998) 1421–1427.
[22] S. Lu, U. Sohling, T. Krajewski, M. Mennig, H. Schmidt, Synthesis and characterization of PbS nanoparticles in ethanolic solution stabilized by hydroxypropylcellulose, J. Mater. Sci. Lett. 17 (1998) 2071–2073.
[23] U. Sohling, G. Jung, D.U. Saenger, S. Lu, B. Kutsch, M. Mennig, Synthesis and optical properties of Mn^{2+}-doped ZnS nanoparticles in solutions and coatings, J. Sol-Gel Sci. Technol. 13 (1998) 685–689.
[24] L.S.C. Wan, P.W.S. Heng, L.F. Wong, The effect of hydroxypropylcellulose on water penetration into a matrix system, Int. J. Pharm. 73 (1991) 111–116.
[25] K. Mitchell, J.L. Ford, D.J. Armstrong, P.N.C. Elliott, C. Rostron, J.E. Hogan, The influence of the particle size of hydroxypropylmethylcellulose K15M on its hydration and performance in matrix tablets, Int. J. Pharm. 100 (1993) 175–179.
[26] E.K. Just, T.G. Majewick, Cellulose ethers, in: F.M. Herman (Ed.), Encyclopedia of Polymer Science and Engineering, Wiley-Interscience, New York, 1990, pp. 226–269.
[27] B. Chankvetadze, M. Saito, E. Yashima, Y. Okamoto, Enantioseparation using selected polysaccharides as chiral buffer additives in capillar electrophoresis, J. Chromatogr. A 773 (1997) 331–338.
[28] S. Koda, T. Hori, H. Nomura, F. Kawaizumi, Hydration of methylcellulose, Polymer 32 (1991) 2806–2810.
[29] L. Robitaille, N. Turcotte, S. Fortin, G. Charlet, Calorimetric study of aqueous solutions of hydroxypropylcellulose, Macromolecules 24 (1991) 2413–2418.
[30] T. Kondo, The relationship between intramolecular hydrogen bonds and certain physical properties of regioselectively substituted cellulose derivatives, J. Polym. Sci. B: Polym. Phys. 35 (1997) 717–723.
[31] D-S. Lee, A.S. Perlin, ^{13}C-NMR spectral and related studies on the distribution of substituents in o-(2-hydroxypropyl)cellulose, Carbohydr. Res. 106 (1982) 1–19.
[32] C. Alvarez-Lorenzo, R. Lorenzo-Ferreira, J.L. Martínez-Pacheco, C. Gómez-Amoza, A. Souto, comparison of gas-liquid chromatography. NMR spectroscopy and Raman spectroscopy for determination of the substituent content of general non-ionic cellulose ethers, J. Pharm. Biomed. Anal. 20 (1999) 375–385.
[33] M.L. Nelson, R.T. O'Connor, Relation of certain infrared bands to cellulose crystallinity and crystal lattice type. Part II. A new inferred ratio for estimation of crystallinity in celluloses I and II, J. Appl. Polymer Sci. 8 (1964) 1325–1341.
[34] E.P. Barrett, L.G. Joyner, P.P. Halenda, The determination of pore volume and area distributions in porous substances, I. Computations from nitrogen isotherms, J. Am. Chem. Soc. 73 (1951) 373–380.
[35] R.C. West, Handbook of Chemistry and Physics, 70th Edition, C.R.C. Press, Boca Raton, FL, 1990, pp. F–6.
[36] S. Malamataris, P. Goidas, A. Dimitrou, Moisture sorption and tensile strength of some tableted direct compression excipients, Int. J. Pharm. 68 (1991) 51–60.
[37] R.C. Rowe, M.D. Parker, D. Bray, Batch and source of variations in excipients, Quantification using microcalorimetry, Pharm. Technol. Eur. 2 (1994) 26–30.

[38] S. Aoki, H. Ando, M. Ishii, S. Watanabe, H. Ozawa, Water behaviour during drug release from a matrix as observed using differential scanning calorimetry, J. Control. Release 33 (1995) 365–374.
[39] K. Mitchell, J.L. Ford, D.J. Armstrong, P.N.C. Elliott, C. Rostron, J.E. Hogan, The influence of substitution type on the performance of methylcellulose and hydroxypropylmethylcellulose in gels and matrices, Int. J. Pharm. 100 (1993) 143–154.
[40] R.E. Walpole, R.H. Myers, Probability and Statistics for Engineers and Scientists, 4th Edition, McMillan, New York, 1985, pp. 463–527.
[41] P. Zadorecki, T. Hjertberg, M. Arwidson, Characterization of cellulose ethers by ^{13}C NMR. 2. Structural determination, Makromol. Chem. 188 (1987) 513–525.
[42] M. Landín, R. Martínez-Pacheco, J.L. Gómez-Amoza, C. Souto, A. Concheiro, R.C. Rowe, Effect of country of origin on the properties of microcristalline cellulose, Int. J. Pharm. 91 (1993) 123–131.
[43] G. Salvetti, E. Tognoni, E. Tombari, G.P. Johari, Excess energy of polymorphic states or glass over the crystal state by heat of solution measurement, Thermochimica Acta 285 (1996) 243–252.
[44] R.G. Zhbankov, Hydrogen bonds and structure of carbohydrates, J. Mol. Struct. 270 (1992) 523–539.
[45] F. Muller-Plathe, Different states of water in hydrogels? Macromolecules 31 (1998) 6721–6723.
[46] C. Alvarez-Lorenzo, J.L. Gómez-Amoza, R. Martínez-Pacheco, C. Souto, A. Concheiro, Microviscosity of hydroxypropylcellulose gels as a basis for prediction of drug diffusion rates, Int. J. Pharm. 180 (1999) 91–103.
[47] I. Katzhendler, R. Azouri, M. Friedman, Crystalline properties of carbamazepine in sustained release hydrophilic matrix tablets based on hydroxypropyl methylcellulose, J. Control. Release 54 (1998) 69–85.
[48] M. Kojima, S. Ando, K. Kataoka, T. Hirota, K. Aoyagi, H. Nakagami, Magnetic resonance imaging (MRI) study of swelling and water mobility in micronized low-substituted hydroxypropylcellulose matrix tablets, Chem. Pharm. Bull. 46 (1998) 324–328.
[49] G.P. Johari, Water's character from dieletric relaxation above its Tg, J. Chem. Phys. 105 (1996) 7079–7082.